2015 IEEE/RSJ International Conference on Intelligent Robots and Systems (IROS)
Congress Center Hamburg
Sept 28 - Oct 2, 2015. Hamburg, Germany

Highly Stretchable Optical Sensors for Pressure, Strain, and Curvature Measurement

Celeste To[1], Tess Lee Hellebrekers[2], and Yong-Lae Park[3]

Abstract— **Recent advances in soft sensors using microfluidic liquid conductors enabled sensing of large deformation of soft structures. However, the use of liquids as conductive media carries a risk of leakage in many cases. Furthermore, it could be harmful when exposed to the human body in certain applications. To address these issues, a different sensing mechanism was proposed: highly stretchable optical sensors that could detect multiple modes of deformation. The method of operation involves a simple waveguide and its housing which are both made of silicone elastomer. The soft waveguide is coated with a thin gold reflective layer to encapsulate light propagating internally, with an light-emitting diode (LED) and a photodiode embedded at each end. When the sensor is stretched, compressed, or bent, micro-cracks within the reflective layer form and allow part of the light to escape, resulting in optical power losses in the light transmission. In this paper, we describe the design and fabrication of the proposed soft sensors. A prototype was created and characterized for pressure, strain, and curvature up to 350 kPa, 90%, and 0.12 mm^{-1}, respectively, showing promising results of reasonable repeatability and linearity in certain ranges.**

I. INTRODUCTION

The advent of soft robotics stemmed from the need of robotic systems that closely interact with human beings with increased safety and friendliness. The materials and methods used in soft robots differ greatly from those in traditional robots that are typically made of rigid materials and structures [1], [2] . One of the most important elements in soft robotics, and also in robotics in general, is the performance of sensors. Soft sensors that have been developed so far have utilized a range of polymer materials, such as Polydimethylsiloxane (PDMS) and other silicone rubbers.

However, most polymers are nonconductive, requiring conductive media that can transmit electric signals through the material without significantly changing the base materials' "soft" properties (i.e., flexibility and stretchability). For this reason, liquid conductors have been one of the most preferred and commonly used mediums due to their continuous property [3], [4], [5]. They can be easily transformed to completely soft electrical wires in highly deformable structures when encapsulated and sealed by a closed microchannel embedded in a soft structure. The microchannels with conductive liquids also work as a sensing element by changing their electrical resistance when the host structure deforms. Many soft sensors have been developed using liquid metals [6], [7] embedded in microchannels for detecting strains and pressures [4], [8], multi-axis shear forces [9], and curvatures [10]. For biocompatibility, nonmetalic liquid conductors, such as ionic liquids [11], have also been used [5], [12], [13] although they tend to be much less conductive.

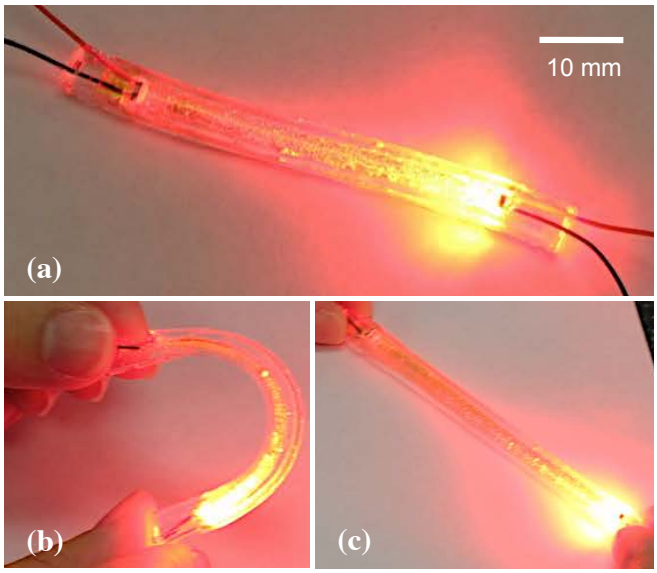

Fig. 1. Optical soft sensor prototype using a stretchable waveguide. (a) Active sensor. (b) Curvature sensing. (c) Strain sensing.

In spite of many advantages of liquid conductors, there are several limitations when they are coupled with soft materials. Encapsulation is one of the major limitations. Liquid conductors are usually injected to a microchannel using a thin syringe needle. Due to the hydrophobic nature of the polymers, the injection requires a relatively high pressure. It is also hard to control the injection pressure since the air captured in the microchannel during fabrication needs to be removed simultaneously. This makes the manufacturing process time-consuming and complicated, requiring complete sealing of the injection ports. There is also a risk of leakage with mechanical failures. This becomes more serious with liquid metals since they could be harmful if they come into contact with the skin or are ingested.

As an alternative to microfluidic sensing, we propose an soft optical sensor, shown in Fig.. 1, for detecting various deformation modes. It is a nontoxic and non-liquid-embedded

[1]Celeste To is with the Department of Mechanical Engineering, Carnegie Mellon University, Pittsburgh, PA 15213, USA (E-mail: cmto@andrew.cmu.edu).

[1]Tess Lee Hellebrekers is with the Department of Mechanical Engineering, University of Texas, Austin, TX 78712, USA (E-mail: tessh@utexas.edu).

[2]Yong-Lae Park is with the Robotics Institute in the School of Computer Science and also with the Department of Mechanical Engineering, Carnegie Mellon University, Pittsburgh, PA 15213, USA (E-mail: ylpark@cs.cmu.edu).

soft sensor that addresses the above issues related to manufacturing complexity while maintaining similar mechanical properties of liquid-phase soft sensors. The idea behind this sensor is to detect light transmission through a reflective waveguide made in a transparent soft material. A mechanical perturbation made to the structure causes a change in the light detected. The novelty is the method of operation in which an inextensible reflective layer is used to achieve the change in the intensity of the light. We also introduce a new transparent, hyperelastic material for the purpose of creating a stretchable waveguide for optical sensing.

Optical sensing is an attractive method due to its immunity to electromagnetic interference, as discussed in various applications [14], [15], [16], and detection of optical power loss combined with optical fibers has been previously used for various sensing applications in flexible structures, such as curvature sensing of a thin biopsy needle [17], shape sensing of a foldable structure [18], and displacement and force sensing in cardiac catheters [19], [20]. However, conventional glass fibers pose a limitation in our application due to their highly limited stretchability. There have been some efforts to provide stretchability to optical sensors using PDMS, one of the most commonly used soft materials in optics due to its optical transparency, low absorption loss, and almost negligible birefringence [21], [22], [23], [24]. Although pressure-sensitive skin for stretchable electronics has been proposed using waveguides in a PDMS layer [25], it was not stretchable enough to measure large deformations due to the limited elongation rate of PDMS.

This paper introduces a hyperelastic sensor capable of detecting multiple modes of deformation: pressure, strain, and curvature. The focus in this work is to demonstrate the feasibility of the proposed novel mechanism: coupling a non-stretchable and a reflective material with a stretchable, optically transparent material. Another objective is to provide simplicity and cleanness in the fabrication that microfluidic sensors have been struggling with. It also aims to reduce manufacturing time and material cost.

II. DESIGN

A. Concept

The method of operation for the proposed sensor, partially inspired by fiber optics, uses the simple notion of transmitting light through a transparent waveguide and detecting the change in its intensity at the other end as the sensor structure undergoes deformation (Fig. 2). The waveguide and the outside housing consist of the same stretchable, transparent elastomer material, and the walls of the waveguide are coated with a thin reflective metal layer. A light source is located at one end of the waveguide, and, at the other end, a photodiode is placed for detecting the light intensity. In principle, the light emitted should be internally reflected and detected at the other end without any loss due to the encapsulating reflective walls (i.e., waveguide). However, as the soft sensor is deformed, many micro-cracks will form within the reflective layer since it is not stretchable. The cracks that form along the channel allow the light to escape,

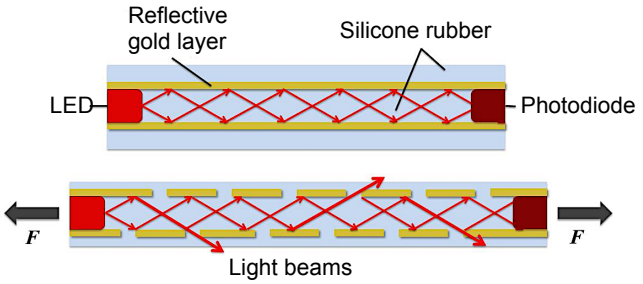

Fig. 2. Principle of operation. (a) Undeformed soft waveguide transmitting light from the source (LED) to the detector (photodiode) through internal reflection without loss. (b) Stretched waveguide with cracks on the reflective gold interface that allow part of light to escape resulting in reduction in light intensity detection.

resulting in a drop in light intensity. This drop can be related to the deformation applied to the sensor. Modes of deformation that we focused on include pressure, stretch, and bending. This sensing mechanism is meant to be simple, clean, and easy to manufacture.

B. Light Intensity Modulation

The main principle of operation for our sensor is light intensity modulation (LTI) [19], [26], [27]. The intensity of light emitted can be modulated when the structure of the sensor is deformed by an external force. We define the measures of the deformations as specifically pressure, strain, and curvature. For light emission and detection, we used a red light-emitting diode (LED) (CREE XLamp XBD) and a photodiode sensitive to red light (Everlight CLS15) with peak wavelength of 625 nm and a peak sensitivity of 620 nm, respectively. Their surface mount form factors are smaller than 3.2 mm facilitated miniaturization of the sensor prototype. The photodiode was operated in forward bias (no-bias) in which a voltage output had a logarithmic relationship with light intensity as following [28].

$$V = \frac{q}{kT}(\ln\frac{i}{i_s} + 1) \tag{1}$$

where V, q, k, T, i, and i_s are voltage output, charge, Boltzman's constant, temperature, current, and saturation current, respectively. We also know that current is linearly proportional to the light intensity. For modeling our system in strain, we can assume that the increase of cracks created within the waveguide is inversely proportional to the light intensity, and the current ratio can be simply replaced by the ratio of the original and stretched surface areas of the waveguide. Assuming the surface area change is dominated by the length change, the ratio further reduces to that of lengths, the original length (l_0) divided by the stretched length (l). Also, we can replace $\frac{q}{kT}$ with our known initial voltage V_0 for simplification. Finally, the theoretical model can be expressed as

$$V = V_0(\ln\frac{l_0}{l} + 1). \tag{2}$$

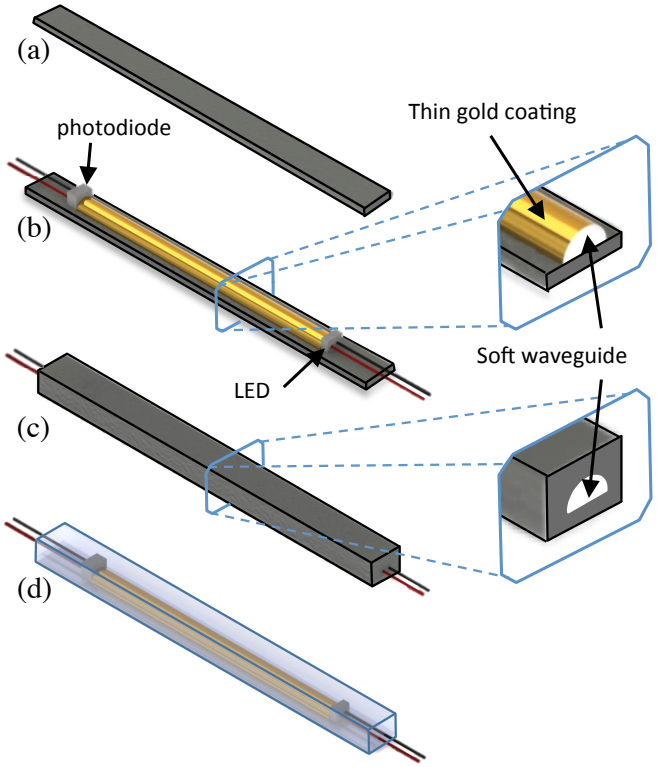

Fig. 3. Fabrication process of soft optical sensor with three steps: (a) silicone rubber is poured in bottom quarter of sensor, (b) add in the transparent waveguide with embedded electronics and (c) completely encapsulate the rest of the sensor. Complete sensor is shown in (d).

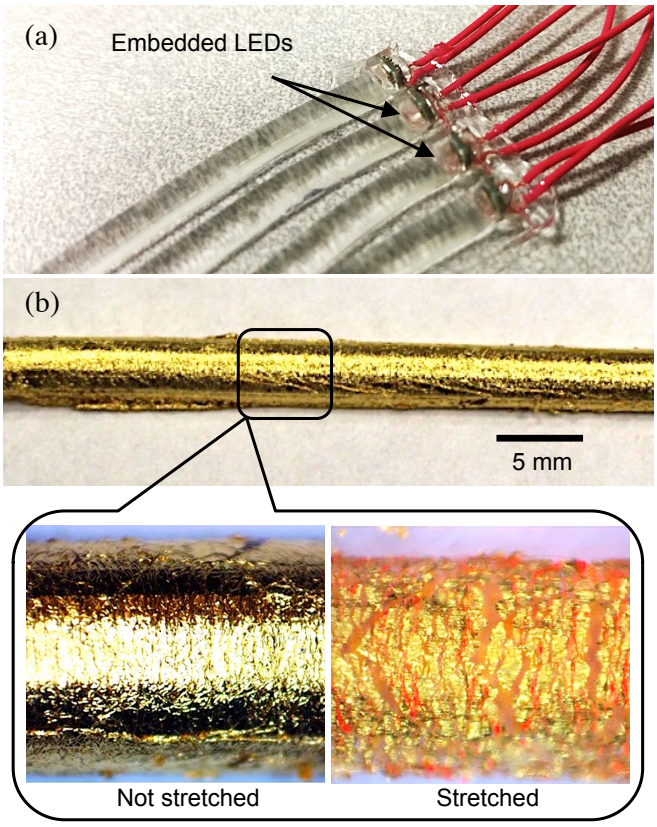

Fig. 4. Soft optical waveguide. (a) Clear elastomer channels with embedded electronics. (b) Optical channel coated with a thin gold layer and its microscopic images of the gold layer showing microcracks when stretched.

C. Waveguide and Housing

PDMS is one of the most commonly used polymer materials compatible with optical elements due to its transparency, as previously discussed in [22], [29], [30]. However, one limitation of typical PDMS is its relatively low elongation at break. Although there are highly stretchable elastomers commercially available, hardly any of them are optically clear. This led us to create a custom hybrid material between PDMS and a silicone gel (EcoFlex Gel, Smooth-On). While PDMS is optically transparent with limited stretchability, the silicone gel is both stretchable and optically clear but too soft and tacky to be used as an independent sensor material. The mixing ratio of the two materials was 9:1 of EcoFlex Gel and PDMS, respectively. The hybrid polymer not only maintained the same optical transparency but also provided high stretchability (elongation at break: approximately 100%). This will be further discussed in Section IV.

While optical fibers achieve total internal reflection using two different refractive indices between the waveguide and the outer cladding, our sensor achieves total internal reflection using a reflective coating between the housing and the waveguide. We used pure (24k) gold leaves (thickness: 0.12 μm) to coat the outside surfaces of the waveguide. Gold was chosen for several reasons: i) gold is biocompatible as previously discussed with medical instruments [17], [20], ii) gold reflects 95% of wavelengths that are longer than 500 nm (e.g. infrared and visible red light) [31], [32], and iii) gold does not tarnish unlike other reflective metals, such as aluminum and silver.

In order to create a sensor that can be comparable to those using liquid conductors, the sensor geometry and size was designed to be as small as possible. The size of the waveguide was accommodated to have a close fit with necessary circuit elements such as an LED and a photodiode. The cross sectional area of the waveguide was chosen to be a semi-circle for simplicity in manufacturing, assuming that the influence of the cross-sectional shape on the internal reflection is negligible.

III. FABRICATION

The fabrication is relatively simple and takes approximately 5 hours at room temperature for a complete prototype. A 9:1 mix of EcoFlex Gel and PDMS was used for the substrate in order to create a highly stretchable and optically transparent silicone hybrid. We added black pigment (Silc Pig, SmoothOn) to the material surrounding the clear waveguide to prevent interference from ambient light. For the final prototype, there was a three-step process for creating the sensor, as shown in Fig. 3. First, two separate molds were used to fabricate the semicircular waveguide and the bottom layer of the sensor (Fig. 3-a). Before curing the waveguide,

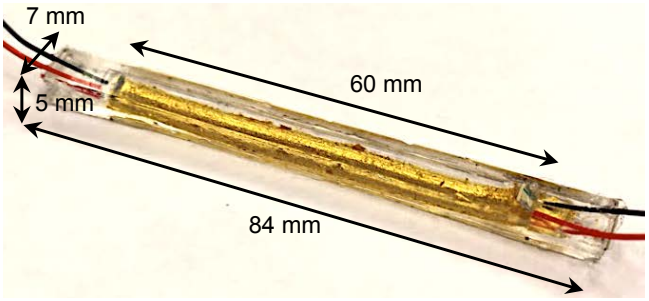

Fig. 5. Complete prototype with dimensions. Clear housing material was used to show the inside of the sensor in this prototype. For an actual working prototype, the housing material is dyed black to prevent signal interference from ambient lights.

an LED and a photodiode were embedded in the opposite ends (Fig. 4-a). After curing, the waveguide was coated in a layer of gold leaf (Fig. 4-b). No extra bonding material was used since the gold adhered well to the naturally tacky substrate. Second, the complete waveguide was placed on top of the bottom layer (Fig. 3-b). Lastly, we poured more substrate to cover the waveguide and complete the sensor (Figs. 3-c and 3-d). For each stage of curing, the molds were placed in a vacuum chamber for 10 minutes and then cured at room temperature for 2 hours.

The final prototype, shown in Fig. 5, is 84 mm long, 7 mm wide, and 5 mm tall. The semicircular waveguide has a diameter of 4 mm and a length of 60 mm. There was an extra 10 mm on each end for clamping for tensile testing, and an extra 4 mm to accommodate the LED and photodiode.

IV. RESULTS

Three modes of deformation (pressure, stretching, and bending) were tested for characterizing the sensor. All three tests were conducted using a motorized materials test stand (ESM301, Mark-10). The output signal for each mode was voltage that was converted from the photocurrent generated by the photodiode.

A. Pressure Response

Pressures up to over 350 kPa were applied in the middle of the sensor structure and until the channel was fully collapsed, as shown in Fig. 6-a. The sensor was constrained at the ends to prevent slip during testing. Three loading rates were tested: 1mm/s, 2 mm/s, and 4 mm/s, and force data were collected using a commercial single-axis load cell (STL-50, AmCells) and divided by the area where the force was applied to calculate the pressure. Each trial went through a complete cycle of loading and unloading in order to check for hysteresis.

The relationship between the signal response and the applied pressure is given in Fig. 7-a. The top part of the curves indicate the sensor output upon loading and the bottom of the curves is during unloading. The signal output was obtained by normalizing the output voltage to the initial voltage of the sensor. Loading rates corresponding to the pressure

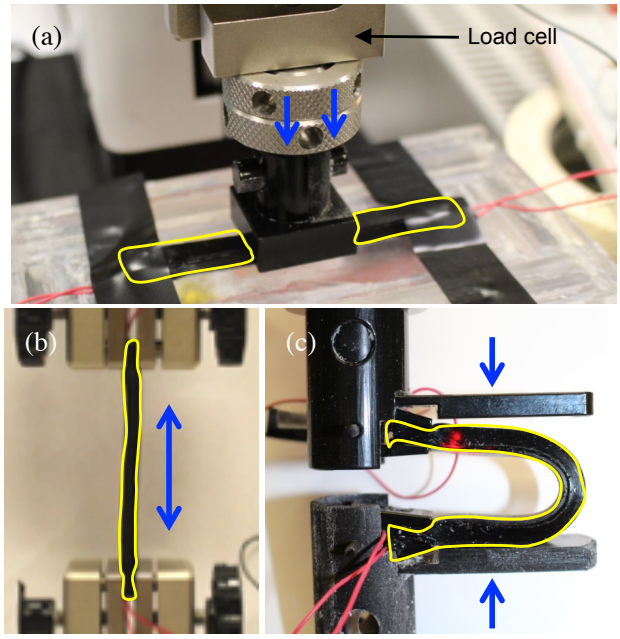

Fig. 6. Experimental setups for three different deformation tests: (a) pressure, (b) strain, and (c) curvature responses. (The yellow outlines show where the sensor is placed within the test beds, and the blue arrows shows the directions of stresses.)

response are shown in blue, green, and red representing 1 mm/s, 2 mm/s, and 4 mm/s, respectively. The output consistency in the loading and unloading indicate that the signal response is not significantly affected by loading rate. However, the discrepancy between the loading and unloading signals slightly increased as the rate increased due to the viscoelastic properties of the silicone rubber hybrid. During the initial loading, the channel will not deform until it reaches a particular threshold. While unloading, the channel takes additional time to regain its original shape. This testing showed a dynamic range of pressure in which the sensor was capable of operating within: 0-200 kPa. After 200 kPa, the signal started to converge to approximately 0.4. This convergence is most likely the reason behind the signal's nonlinearity.

B. Strain Response

In this test, loading a sensor axially between clamps, the gauge length was measured and used to calculate the engineering strain (Fig 6-b). Using three different loading rates (1 mm/s, 2 mm/s, and 4 mm/s), the sensor was loaded and unloaded. The sensor was loaded up to over 90% strain, safely below the failure strain level (approximately 100%) measured in a separate experiment, which will be discussed later (Section IV-D). One sensor was subjected to a cycle of loading and unloading at three different loading rates, shown in Fig. 7-b. The response demonstrates that the signal is independent of strain rate. Hysteresis was hardly observed at lower rates (1 mm/s and 2 mm/s). However, as the rate increased to 4 mm/s, it started to show due to the viscoelastic properties of the sensor material.

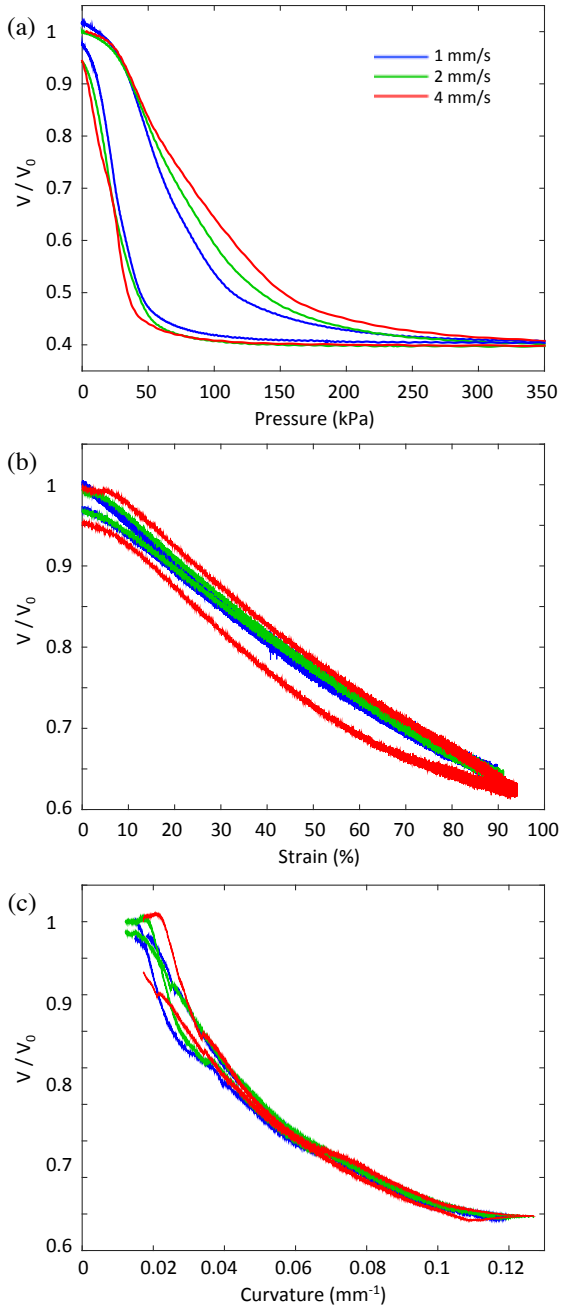

Fig. 7. (a) Pressure response. (b) Strain Response. (c) Curvature Response.

C. Curvature Response

Testing for the curvature response involved a set of custom-built clamps for inducing buckling on the sensor, as shown in Fig. 7-c. Since the chord and arc length are known, the radius of curvature can be calculated. The curvature increased with the output signal in a predictable pattern. It should be noted, however, that the test set-up was not perfect, and was not able to evenly bend the sensor. While this introduced some unexpected peaks in the data, the overall relationship between the output and curvature is clear and promising.

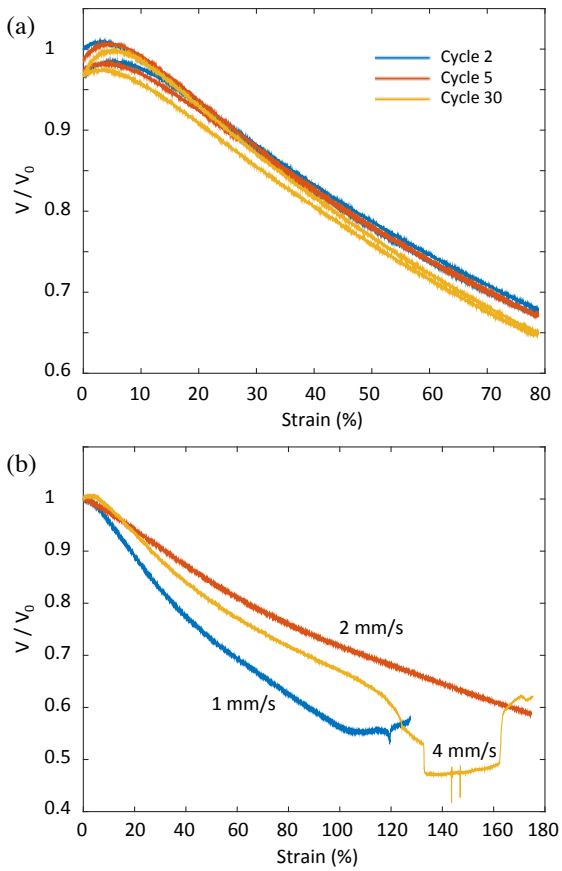

Fig. 8. (a) Cyclic test result. (b) Failure test result.

D. Cyclic and Failure Tests for Strain

In addition to the basic characterization tests shown above, failure and cyclic tests were conducted to evaluate the robustness and repeatability of the sensor.

For the cyclic test, one sensor sample was clamped in the test stand and stretched and released for three different cycles at a rate of 2 mm/s. The results from cycles 2, 5, and 30 are shown superimposed in Fig. 8-a. These results demonstrate the sensor's consistency over time.

For the failure test, three sensor samples were stretched using three different loading rates (1 mm/s, 2 mm/s, and 4 mm/s) until the sensors mechanically failed. The failure was detected by the sensor signal, as shown in Fig. 8-b. All three sensors were able to tolerate over 100% strain.

V. DISCUSSION

This sensor type was meant to provide an easy manufacturing methods with materials that would be easily accessible. However, we are looking to improve the reflective layer in a more robust sensor in which we will be using sputter deposition to apply the reflective layer. This will be beneficial because it ensures a uniform coating throughout the surface of the channel - the thickness may not be uniform however. The next area of improvement would be the substrate itself. It was difficult searching for a highly stretchable material that

was optically transparent as well. In result of this, a hybrid between the aforementioned silicone rubbers was created. However, this means the material properties are unknown even though we know some of the properties from each individual polymer. We were able to determine the elongation at break for the sensors. We will further characterize the material itself to have more complete data, such as shore hardness, and elastic modulus.

As for future developments, we are currently working on two extended sensor types. The first is a multi-modal sensor by having multiple sensors integrated in one sensor block using the same principle of operation. The sensor would be able to discern various modes of deformation, such as compression, bending, and twisting. The second extension is to use optical fibers at each end to transmit and detect light through the soft waveguide instead of directly embedding a light source and a detector in the soft material. Optical fibers will allow us not only to further minimize the size of the sensor but also to simplify the manufacturing process by removing multiple rigid components, such as LEDs, and photodiodes, at the test bed.

VI. CONCLUSION

A soft optical sensor, highly stretchable and flexible, was designed, fabricated, and characterized. The pressure, strain, and curvature responses showed promising results with near-linear and repeatable signals. This demonstrated the potential to replace or act as a substitute for microfluidic soft sensors. In addition, the simplicity of manufacturing makes this method much more feasible.

REFERENCES

[1] S. Kim, C. Laschi, and B. Trimmer, "Soft robotics: a bioinspired evolution in robotics," *Trends Biotechnol.*, vol. 31, no. 5, pp. 287–294, 2013.

[2] C. Majidi, "Soft robotics: a perspective–current trends and prospects for the future," *Soft Rob*, vol. 1, no. 1, pp. 5–11, 2014.

[3] Y.-L. Park, C. Majidi, R. Kramer, P. Berard, and R. J. Wood, "Hyperelastic pressure sensing with a liquid-embedded elastomer," *J. Micromech. Microeng.*, vol. 20, no. 12, p. 125029, 2010.

[4] Y.-L. Park, B. Chen, and R. J. Wood, "Design and fabrication of soft artificial skin using embedded microchannels and liquid conductors," *IEEE Sens. J.*, vol. 12, no. 8, pp. 2711–2718, 2012.

[5] C.-Y. Wu, W. H. Liao, and Y.-C. Tung, "Integrated ionic liquid-based electrofluidic circuits for pressure sensing within polydimethylsiloxane microfluidic systems," *Lab Chip*, vol. 11, no. 207890, pp. 1740–1746, 2011.

[6] M. D. Dickey, R. C. Chiechi, R. J. Larsen, E. a. Weiss, D. a. Weitz, and G. M. Whitesides, "Eutectic gallium-indium (EGaIn): A liquid metal alloy for the formation of stable structures in microchannels at room temperature," *Advanced Functional Materials*, vol. 18, pp. 1097–1104, 2008.

[7] T. Liu, P. Sen, and C. Kim, "Characterization of nontoxic liquid-metal alloy galinstan for applications in microdevices," *J. Microelectromech. Syst.*, vol. 21, pp. 443–450, 2012.

[8] R. P. Wong, J. Posner, and V. Santos, "Flexible microfluidic normal force sensor skin for tactile feedback," *Sens. Actuators, A*, vol. 179, pp. 62–69, 2012.

[9] D. M. Vogt, Y.-L. Park, and R. J. Wood, "Design and Characterization of a Soft Multi-Axis Force Sensor Using Embedded Microfluidic Channels," *IEEE Sensors Journal*, vol. 13, no. 10, pp. 4056–4064, Oct. 2013.

[10] C. Majidi, R. Kramer, and R. J. Wood, "A non-differential elastomer curvature sensor for softer-than-skin electronics," *Smart Mater. Struct.*, vol. 20, p. 105017, 2011.

[11] A. Visser, N. Bridges, and R. Rogers, *Ionic Liquids: Science and Applications*. American Chemical Society, 2012, vol. 1117.

[12] J.-B. Chossat, Y.-L. Park, R. J. Wood, and V. Duchaine, "A Soft Strain Sensor Based on Ionic and Metal Liquids," *IEEE Sens. J.*, vol. 13, no. 9, pp. 3405–3414, Sept. 2013.

[13] J.-B. Chossat, H.-S. Shin, Y.-L. Park, and V. Duchaine, "Design and Manufacturing of Soft Tactile Skin using an Embedded Ionic Liquid and Tomographic Imaging," *J Mech Robot*, no. c, 2014.

[14] K. Li, I.-M. Chen, S. H. Yeo, and C. K. Lim, "Development of finger-motion capturing device based on optical linear encoder," *J. Rehabil. Res. Dev.*, vol. 48, no. 1, p. 69, 2011.

[15] P. Kampmann and F. Kirchner, "Integration of fiber-optic sensor arrays into a multi-modal tactile sensor processing system for robotic end-effectors." *Sensors*, vol. 14, no. 4, pp. 6854–76, Jan. 2014.

[16] A. Grillet, D. Kinet, J. Witt, M. Schukar, K. Krebber, F. Pirotte, and A. Depré, "Optical fiber sensors embedded into medical textiles for healthcare monitoring," *IEEE Sens. J.*, vol. 8, no. 7, pp. 1215–1222, 2008.

[17] S. C. Ryu, Z. F. Quek, P. Renaud, R. J. Black, B. L. Daniel, and M. R. Cutkosky, "An optical actuation system and curvature sensor for a MR-compatible active needle," in *Proc. IEEE Int. Conf. Rob. Autom. (ICRA'12)*. Ieee, May 2012, pp. 1589–1594.

[18] M. K. Dobrzynski, I. Halasz, R. Pericet-camara, D. Floreano, and S. Member, "Contactless deflection sensing of concave and convex shapes assisted by soft mirrors," in *Proc. IEEE/RSJ Int. Conf. Intell. Rob. Syst. (IROS'12)*, 2012, pp. 4810–4815.

[19] P. Polygerinos, A. Ataollahi, T. Schaeffter, R. Razavi, L. D. Seneviratne, and K. Althoefer, "Mri-compatible intensity-modulated force sensor for cardiac catheterization procedures," *IEEE Trans. Biomed. Eng.*, vol. 58, no. 3, pp. 721–6, Mar. 2011.

[20] P. Polygerinos, L. D. Seneviratne, R. Razavi, T. Schaeffter, and K. Althoefer, "Triaxial catheter-tip force sensor for MRI-guided cardiac procedures," *IEEE/ASME Trans. Mechatron.*, vol. 18, no. 1, pp. 386–396, Feb. 2013.

[21] H. Ma, a.K. Y. Jen, and L. Dalton, "Polymer-Based Optical Waveguides: Materials, Processing, and Devices," *Adv. Mater.*, vol. 14, no. 19, pp. 1339–1365, Oct. 2002.

[22] S. Kopetz, D. Cai, E. Rabe, and A. Neyer, "PDMS-based optical waveguide layer for integration in electrical–optical circuit boards," *AEU Int. J. Electron. Commun*, vol. 61, no. 3, pp. 163–167, Mar. 2007.

[23] D. Cai, a. Neyer, R. Kuckuk, and H. Heise, "Optical absorption in transparent PDMS materials applied for multimode waveguides fabrication," *Opt. Mater.*, vol. 30, no. 7, pp. 1157–1161, Mar. 2008.

[24] Y. Fainman, *Optofluidics: Fundamentals, Devices, and Applications*. Yeshaiahu Fainman, 2009, ch. 2. Basic Microfluidic and Soft Lithographic Techniques, pp. 7–32.

[25] M. Ramuz, B. C.-K. Tee, J. B.-H. Tok, and Z. Bao, "Transparent, optical, pressure-sensitive artificial skin for large-area stretchable electronics." *Adv. Mater.*, vol. 24, no. 24, pp. 3223–7, June 2012.

[26] P. Polygerinos, L. D. Seneviratne, and K. Althoefer, "Modeling of light intensity-modulated fiber-optic displacement sensors," *IEEE Trans. Instrum. Meas.*, vol. 60, no. 4, pp. 1408–1415, Apr. 2011.

[27] P. Puangmali, K. Althoefer, and L. D. Seneviratne, "Mathematical modeling of intensity-modulated bent-tip optical fiber displacement sensors," *IEEE Trans. Intrum. Meas.*, vol. 59, no. 2, pp. 283–291, 2010.

[28] J. Fraden, *Handbook of Modern Sensors*, 3rd ed. New York: Springer-Verlag, 2004.

[29] D. Chang-Yen, R. Eich, and B. Gale, "A monolithic PDMS waveguide system fabricated using soft-lithography techniques," *Journal of Lightwave Technology*, vol. 23, no. 6, pp. 2088–2093, June 2005.

[30] J. S. Kee, D. P. Poenar, P. Neuzil, and L. Yobas, "Monolithic integration of poly(dimethylsiloxane) waveguides and microfluidics for on-chip absorbance measurements," *Sens. Actuators, B*, vol. 134, no. 2, pp. 532–538, Sept. 2008.

[31] J. N. Hodgson, "The optical properties of gold," *J. Phys. Chem. Solids*, vol. 29, pp. 2175–2181, 1968.

[32] O. Loebich, "The optical properties of gold," *Gold Bulletin*, vol. 5, pp. 2–10, 1972.

[33] Y.-L. Park, D. Tepayotl-Ramirez, R. J. Wood, and C. Majidi, "Influence of cross-sectional geometry on the sensitivity of liquid-phase electronic pressure sensors," *Appl. Phys. Lett.*, vol. 101, no. 19, 2012.